Additivity of Cation−π Interactions: An ab Initio Computational Study on π−Cation−π Sandwich Complexes

Tong Liu,[†] Weiliang Zhu,*[†,‡] Jiandu Gu,[†] Jianhua Shen,*[,†] Xiaomin Luo,[†] Gang Chen,[‡] Chum Mok Puah,[‡] Israel Silman,[§] Kaixian Chen,[†] Joel L. Sussman,[||] and Hualiang Jiang*[,†]

Center for Drug Discovery and Design, State Key Laboratory of New Drug Research, Shanghai Institute of Materia Medica, Shanghai Institutes of Biological Sciences, Chinese Academy of Sciences, 555 Zu Chong Zhi Road, Shanghai, 201203, P. R. China, Technology Centre for Life Sciences, Singapore Polytechnic, 500 Dover Road, Singapore 139651, Department of Neurobiology, Weizmann Institute of Science, 76100 Rehovot, Israel, and Department of Structural Biology, Weizmann Institute of Science, 76100 Rehovot, Israel

Received: May 28, 2004; In Final Form: August 6, 2004

The π−cation−π interaction between a cation or a cationic group and several aromatic residues, although rather prevalent in biological systems, has not been studied theoretically. The ab initio MP2 calculations were carried out on the systems composed of TMA with two aromatic rings, viz. benzene, pyrrole, or indole, to explore how a cation or a cationic group interacts simultaneously with two aromatic residues in proteins or nucleic acids. The calculated results on π−TMA−π complexes revealed additivities of both the geometries and the binding energies relative to cation−π complexes. The preferred structure of such a complex can be constructed by superimposing the corresponding TMA−π complexes via the cation. The binding energies of the π−TMA−π sandwiches are the sums of the two corresponding TMA−π systems. The contribution of electron correlation to the overall binding energy is estimated to be at least 50%, with dispersion serving as the main component of the electron correlation interaction. Similar to geometrical and energetic additivity, the additivities in BSSE and ΔZPE were also found. Therefore, our finding provides a convenient and effective way to construct π−TMA−π sandwiches and to estimate their binding energies. Morokuma decomposition analysis on the binding energy indicated that the electrostatic, charge transfer, and polarity interactions drive the binding of TMA with aromatics, whereas the exchange repulsion and high order coupling always obstruct the TMA approaching aromatics. Charge-transfer happens to some extent during the complexation of TMA with aromatics, and the transferred NPA atomic charges and charge-transfer energies are almost same in different complexes of TMA−π or π−TMA−π. The interaction between the 2 aromatics in the sandwich π−TMA−π complexes is negligible because of their long interaction distances. All this information should be helpful in studying such interactions in biological systems.

1. Introduction

The interaction between a cation and an aromatic ring, termed the cation−π interaction, is of importance in molecular recognition and protein folding.[1−3] The X-ray structure of a choline-binding domain in LytA (PDB code 1HCX) revealed that the cation−π interaction between the quaternary moiety of the bound choline and aromatic residues of the protein is crucial for the stabilization of its structure.[4] The distances between the nitrogen atom of the choline and the two planes of the indoles of Trp241 and Trp248 are ∼4.5 Å, and the dihedral angle between the two indoles is 71°. Other protein crystal structures have also been described in which several aromatic residues surround a cation. For example, Aleshin et al.[5] found that in the crystal structure of glucoamylase, the protonated Lys108 is surrounded by two tryptophans and two tyrosines, an example of the interaction of a cation with as many as four aromatic rings. The crystal structure of the K^+ channel shows that the mouth of the extracellular entrance is composed of the aromatic rings of four conserved tyrosines.[6] Electrophysiological data suggest that the mechanism of blocking of the channel by quaternary ammonium moieties involves interaction with four phenol groups.[6] Thus, both structural and functional data show that a single cation may interact simultaneously with more than one aromatic ring. In fact, a survey of available protein structures showed that ca. 50% of all arginine residues are in contact with two aromatic side chains.[7] Thus, the interaction between a cation and two aromatic rings, which we term a π−cation−π sandwich interaction, is quite prevalent and may be expected to play significant roles both in maintaining protein structures and in protein−cation interactions.

Little research has been devoted to π−cation−π sandwiches relative to the extensive studies performed for the simpler cation−π interaction.[8−12] Certain critical issues need to be addressed: Specifically, do π−cation−π sandwiches possess characteristics similar to those of cation−π systems, thus permitting extension to the former of conclusions reached from the extensive studies on the latter, and how can the binding strength of interaction of a cation with more than one aromatic group be calculated? To answer these questions, we carried out a theoretical study on several π−cation−π sandwiches.

* To whom correspondence should be addressed. E-mail: hljiang@mail.shcnc.ac.cn. Tel: +86-21-50807188. Fax: +86-21-50807088.
[†] Chinese Academy of Sciences.
[‡] Singapore Polytechnic.
[§] Weizmann Institute of Science.
[||] Weizmann Institute of Science.

10.1021/jp0476850 CCC: $27.50
Published on Web 10/01/2004

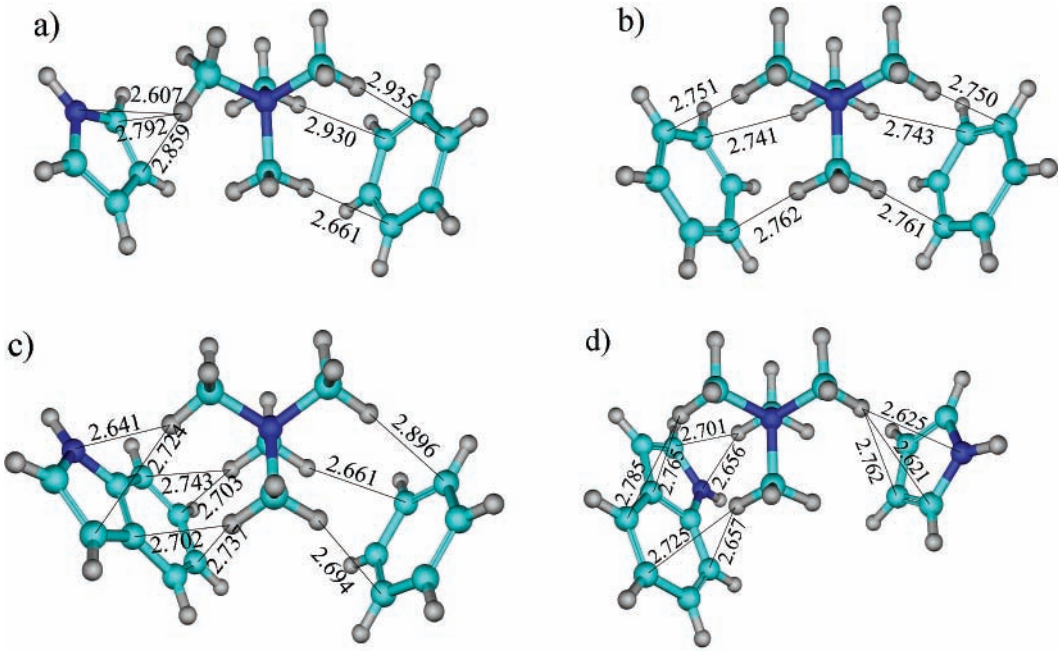

Figure 1. Optimized structures of π−TMA−π sandwiches: (a) benzene−TMA−pyrrole; (b) benzene−TMA−benzene; (c) benzene−TMA−indole; (d) pyrrole−TMA−indole.

2. Computational Details

The aromatics studied were benzene, pyrrole, and indole, corresponding to the aromatic side chains of three natural amino acids. The cation employed was tetramethylammonium (TMA), which is structurally homologous to a broad repertoire of protein ligands and substrates. Twelve initial π−TMA−π sandwiches were selected (Figure S1, Supporting Information) and were optimized at the MP2/6-31G* level. The binding energy, ΔE, between TMA and two aromatics, $\pi 1$ and $\pi 2$, was calculated at the MP2/6-31+G**//MP2/6-31G* level using

$$\Delta E = E_{\pi 1-\mathrm{TMA}-\pi 2} - (E_{\pi 1} + E_{\mathrm{TMA}} + E_{\pi 2}) \qquad (1)$$

It was then corrected by both the basis set superposition error (BSSE) and the zero-point energy (ZPE)

$$\Delta E^{\mathrm{corr}} = \Delta E + \mathrm{BSSE} + \Delta \mathrm{ZPE} \qquad (2)$$

The BSSE was estimated by using[13]

$$\mathrm{BSSE} = [E_{\mathrm{TMA}} - E_{\mathrm{TMA}(\pi 1-\mathrm{TMA}-\pi 2)}] + [E_{\pi 1\pi 2} - E_{\pi 1\pi 2(\pi 1-\mathrm{TMA}-\pi 2)}] \qquad (3)$$

where $E_{\mathrm{TMA}(\pi 1-\mathrm{TMA}-\pi 2)}$ (or $E_{\pi 1\pi 2(\pi 1-\mathrm{TMA}-\pi 2)}$) is the energy of fragment TMA (or $\pi 1\pi 2$), based on the geometry extracted from the optimized structure, with its own basis set augmented by the basis set of $\pi 1\pi 2$ (or TMA). E_{TMA} (or $E_{\pi 1\pi 2}$) is the energy of isolated fragment TMA (or $\pi 1\pi 2$), with just its own basis set.

The calculation was performed using Gaussian98 software on a SGI Power Challenge supercomputer.[14] The ZPE was estimated at the HF/6-31+G** level on the basis of the HF/6-31+G** optimized structure.

Morokuma decomposition analysis on binding energy was carried out at the HF/6-31+G**//MP2/6-31G* level by using the software GAMESS on Pentium IV PCs, to investigate the factors affecting the binding between TMA and aromatics.

3. Results and Discussions

3.1. Additivity in Complex Geometry. Four optimized structures thus obtained at the MP2/6-31G* level are displayed in Figure 1. The interactions between TMA and each aromatic ring in the π−TMA−π system are accomplished principally via three H atoms, each from one of the three methyl groups of the TMA, a finding very similar to that reported for TMA−π structures.[8,9,12] Table 1 summarizes the geometrical calculated parameters.

TABLE 1: Calculated Geometrical Parameters for π−TMA−π Sandwiches and TMA−π Complexes at the MP2/6-31G* Level (Distances in Å and Angles in deg)

system	$d_{\mathrm{N-B}}{}^a$	$d_{\mathrm{N-P}}{}^b$	$d_{\mathrm{N-I}}{}^c$	α^d
Figure 1a, benzene−TMA−pyrrole	4.251	4.169		70.2
Figure 1b, benzene−TMA−benzene	4.245			70.8
Figure 1c, benzene−TMA−indole	4.255		4.025	75.5
Figure 1d, pyrrole−TMA−indole		4.177	4.024	72.8
TMA−pyrrole		4.155		
TMA−benzene	4.230			
TMA−indole			4.011	

[a] Distance between the N of TMA and the plane of the benzene ring. [b] Distance between the N of TMA and the plane of the pyrrole ring. [c] Distance between the N of TMA and the plane of the indole ring. [d] Angle between the two aromatic planes.

The perpendicular interaction distances between TMA and the aromatic rings, d, in Table 1, are elongated by ≤ 0.02 Å in the π−TMA−π sandwiches relative to the corresponding distances in simple TMA−π complexes.[8,9,12] No other significant geometrical differences are observed. Thus, the structural unit of TMA−π in the π−TMA−π sandwich is almost the same as in the stand-alone TMA−π complex, suggesting an additivity permitting the π−TMA−π sandwich to be considered as being derived from the two corresponding TMA−π complexes by overlapping the C, H, and N atoms of their TMA groups.

The optimized π−TMA−π sandwiches resemble those seen in X-ray structures of proteins, inasmuch as the two aromatic rings are not parallel.[1,3,4] This may be attributed to the electrostatic potentials of the aromatics and of TMA, shown in Figure 2, which were created using the DS ViewerPro software.[15] The positively charged areas on the surface of TMA correspond to the H atoms of the methyl groups, whereas the negatively charged areas of the aromatic moieties are located on their rings. Because TMA possesses tetrahedral geometry,

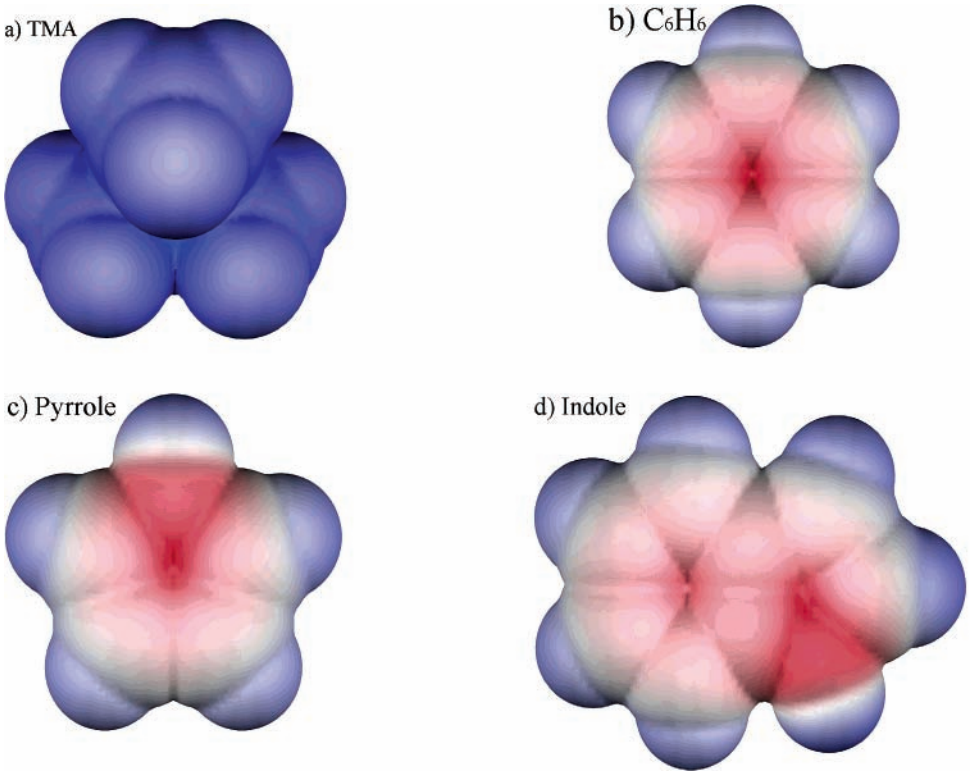

Figure 2. Electrostatic potentials on the van de Waals surfaces of TMA and aromatic rings. The more intense the red color, the greater the negative surface potential; the more intense the blue color, the higher the positive potential.

binding to two aromatic rings via two faces of the tetrahedron should optimize the electrostatic interactions, resulting in a divergent geometry resembling those observed experimentally. Indeed, the angle between the two aromatic planes in an optimized $\pi-$TMA$-\pi$ sandwich, α in Table 1, is found to be very close to the angle between the two faces of a tetrahedron that is 70.5°. For example, this angle is 70.8° and 70.2° in benzene−TMA−benzene and benzene−TMA−pyrrole sandwiches, respectively. Moreover, such a binding model, as discussed below, favors a dispersion interaction.

3.2. Additivity in Binding Strength. The calculated energy parameters at different levels were summarized in Table 2. Table 2a shows that the BSSE- and ΔZPE-corrected binding energy, ΔE^{corr}, for the benzene−TMA−pyrrole sandwich in Figure 1a, is −16.29 kcal·mol^{-1}, a value similar to the sum of the binding energies for TMA−pyrrole, −9.26 kcal/mol, and for TMA−benzene, −7.52 kcal/mol. The same holds true for the other $\pi-$TMA$-\pi$ sandwiches in Figures 1b−d, the ΔE^{corr} values being equal to the sum of the binding energies for the two corresponding TMA$-\pi$ systems within an error of 0.7 kcal/mol, Table 2a. This result suggests that the binding energy between TMA and two aromatics could be easily estimated as the sum of the binding energies of two corresponding stand-alone TMA$-\pi$ complexes, indicating the additivity of both geometry and binding energy in $\pi-$TMA$-\pi$ sandwiches. This same additivity is also found in those binding energies calculated at B3LYP/6-31+G**//MP2/6-31G* and HF/6-31+G**//MP2/6-31G* levels, Table 2b.

The calculated BSSE values at MP2/6-31+G**//MP2/6-31G* level are quite large relative to whole binding energies, Table 2a. The percentage of BSSE over ΔE^{corr} is always higher than 37% and could be as high as 43% in the sandwich of benzene−TMA−indole. Therefore, similar to the case for the simple TMA$-\pi$ complex, it is also an essential step to carry out BSSE correction for $\pi-$TMA$-\pi$ complexes.[16] Furthermore, Table 2a reflects another additivity that the BSSE for the $\pi-$TMA$-\pi$ sandwich is a sum of the BSSEs for the two corresponding stand-alone TMA$-\pi$ complexes. The biggest error in additivity of BSSE is only 8.73 − (3.00 + 4.94) = 0.79 kcal/mol in the case of the complex benzene−TMA−indole. In comparison with the MP2 BSSE, the BSSEs calculated at B3LYP/6-31+G**//MP2/6-31G* and HF/6-31+G**//MP2/6-31G* levels are quite small, which are less than 1.5 kcal/mol in all sandwich complexes (Table 2b).

No imaginary frequency at the HF/6-31+G** level was found from the frequency calculation, suggesting that all optimized geometries at HF/6-31+G** level are reasonable (Supporting Information, Figures S2 and S3). The estimated ΔZPE at the HF/6-31+G**//HF/6-31+G** level for the sandwiches is quite small in comparison with the overall binding energy and with MP2 BSSE correction. It ranges from 0.9 to 1.2 kcal/mol (Table 2). Meanwhile, the additivity in ΔZPE also exists. The error for the ΔZPE additivity is always less than 0.30 kcal/mol, Table 2a. For example, the ΔZPE in the complex benzene−TMA−benzene is 0.91 kcal/mol, and that in the complex TMA−benzene is 0.49 kcal/mol, very close to half of the former with a difference of 0.03 kcal/mol.

It is recognized that the HF theory cannot deal properly with electron correlation, and that the B3LYP method does not take into account the dispersion interaction.[17,18] Thus, the difference in ΔE^{corr} between the HF and MP2 methods can be roughly viewed as the contribution of the electron correlation (E_{e-c}),[17] whereas the difference between the DFT-B3LYP and MP2 methods can be approximately regarded as the contribution of the dispersion interaction (E_{disp}).[18] The contributions of E_{e-c} and E_{disp} in the benzene−TMA−pyrrole sandwich are estimated to be −8.70 and −6.67 kcal/mol, respectively, suggesting that dispersion is a dominant component of the electron correlation. Accordingly, dispersion makes an important contribution to the binding of TMA to aromatic rings. Similar contributions were

TABLE 2: Calculated Energetic Parameters for π−TMA−π Sandwiches and for TMA−π Complexes (E^{MP2}, E^{DFT}, and E^{HF} Energies in Hartree, Others in kcal/mol)

(a) At the MP2/6-31+G**//MP2/6-31G* Level

system	E^{MP2} [a]	BSSE[b]	ΔZPE[c]	ΔE^{corr} [d]	E_{e-c} [e]	E_{disp} [f]
Figure 1a, benzene−TMA−pyrrole	−654.54297	5.99	1.10	−16.29	−8.70(53%)	−6.67(41%)
Figure 1b, benzene−TMA−benzene	−676.52140	6.16	0.91	−14.87	−8.82(59%)	−7.14(48%)
Figure 1c, benzene−TMA−indole	−807.73059	8.73	1.07	−19.55	−12.53(64%)	−10.42(53%)
Figure 1d, pyrrole−TMA−indole	−785.75177	8.27	1.24	−21.04	−12.03(57%)	−9.80 (47%)
TMA−pyrrole	−423.01574	2.91	0.69	−9.26	−5.24 (57%)	−3.08 (33%)
TMA−benzene	−444.99351	3.00	0.49	−7.52	−4.93 (66%)	−3.25 (43%)
TMA−indole	−576.20029	4.94	0.80	−11.33	−6.87 (61%)	−4.81 (42%)
TMA	−213.46550					
pyrrole	−209.52974					
benzene	−231.51047					
indole	−362.70785					

(b) At the B3LYP/6-31+G**//MP2/6-31G* and HF/6-31+G**//MP2/6-31G* Levels

system	ΔZPE[c]	E^{DFT} [g]	BSSE[h]	ΔE^{corr} [d]	E^{HF} [i]	BSSE [j]	ΔE^{corr} [d]
Figure 1a, benzene−TMA−pyrrole	1.10	−656.64481	0.83	−9.62[g]	−652.26341	1.07	−7.59[g]
Figure 1b, benzene−TMA−benzene	0.91	−678.72143	1.04	−7.73[g]	−674.15673	1.03	−6.05[g]
Figure 1c, benzene−TMA−indole	1.07	−810.29879	1.45	−9.13[g]	−804.92991	1.44	−7.02[g]
Figure 1d, pyrrole−TMA−indole	1.24	−788.22267	1.36	−11.24[g]	−783.03923	1.45	−9.01[g]
TMA−pyrrole	0.69	−424.37419	0.43	−5.98	−421.53800	0.528	−4.14
TMA−benzene	0.49	−446.45076	0.49	−4.26	−443.42951	0.455	−2.77
TMA−indole	0.80	−578.02928	0.80	−6.29	−574.20398	0.780	−4.48
TMA		−214.17897			−212.70321		
pyrrole		−210.18391			−208.82626		
benzene		−232.26352			−230.72040		
indole		−363.83773			−361.49112		

[a] MP2 energy at the MP2/6-31+G**//MP2/6-31G* level. [b] BSSE correction at MP2/6-31+G**//MP2/6-31G* level. [c] ΔZPE correction at HF/6-31+G**//HF/6-31+G** level. [d] BSSE- and ΔZPE- corrected binding energy. [e] Estimated electron correlation energy, the value in parentheses being the percentage contribution of E_{e-c} to ΔE^{corr}. [f] Estimated dispersion energy, the value in parentheses being the percentage contribution of E_{disp} to ΔE^{corr}. [g] DFT energy at the DFT-B3LYP/6-31+G**//MP2/6-31G* level. [h] BSSE correction at the B3LYP/6-31+G**//MP2/6-31G* level. [i] RHF energy at the HF/6-31+G**//MP2/6-31G* level. [j] BSSE correction at the HF/6-31+G**//MP2/6-31G* level.

TABLE 3: Calculated ΔZPE at Different Levels

method	benzene−TMA−pyrrole, Figure 1a	TMA−indole
B3LYP/6-31+G*//HF/6-31+G**	1.04	0.97
B3LYP/6-31+G**//HF/6-31+G**	1.04	0.87
B3LYP/6-31G**//B3LYP/6-31G**	1.44	0.80
HF/6-31+G**//HF/6-31+G**	1.10	0.64
HF/6-31G//HF/6-31G		0.64
HF/6-31G*//HF/6-31G*		0.78
HF/6-31G**//HF/6-31G**		0.75
HF/6-311G**//HF/6-311G**		0.69

estimated for the other sandwich complexes studied. Thus the percentage contribution of E_{e-c} to ΔE^{corr} is 53−64%, and of E_{disp} to ΔE^{corr} 41−53%. Furthermore, the E_{e-c} and E_{disp} values are also additive, Table 2a.

On the other hand, as our studied systems are rather big, it is difficult to carry out vibrational analysis by using the MP2 method. Although we thought that, in general, the differences in ΔZPE values calculated using different methods, and the effect of basis sets on these differences should be small, the concern is that, in the case of our studied systems, how great is the difference if the ΔZPE calculated by the Hartree−Fock method is used to describe the ΔZPE of MP2 method, and how different basis sets affect ΔZPE. To clarify this doubt, B3LYP/6-31+G**//HF/6-31+G*, B3LYP/6-31+G*//HF/6-31+G*, and B3LYP/6-31G**//B3LYP/6-31G** calculations were performed for benzene−TMA−pyrrole and for TMA−indole complexes, to test how the different methods affect ΔZPE values. And the HF/6-31G, HF/6-31G*, HF/6-31G**, and HF/6-311G** calculations were carried out for TMA−indole to test how the basis sets affect ΔZPEs. The calculated ΔZPEs were summarized in Table 3. As expected, the difference between the ΔZPE values obtained by using different basis sets and methods for the sandwich benzene−TMA−pyrrole is only ∼0.4 kcal/mol. And the differences in ΔZPEs among different basis sets for the complex TMA−indole are ∼0.3 kcal/mol. We think that the difference between Hartree−Fock and MP2 methods in ΔZPE should be around this range. Therefore, our calculation strategy for ΔZPE calculation should be reasonable, and the estimated binding strength should be reliable.

It was estimated by Rappe that the dispersion contribution made by each first-row atomic pair to binding energy is ∼0.5 kcal/mol.[18] Thus, the order E_{disp}(Figure 1a) ≅ E_{disp}(Figure 1b) < E_{disp}(Figure 1c) ≅ E_{disp}(Figure 1d) is plausible, because the latter two contribute more interactive atomic pairs, and hence a greater E_{disp} to the overall binding energy. This might be an additional reason the π−TMA−π sandwiches display a divergent conformation rather than parallel orientation of the aromatic rings.

3.3. Charge Transfer. The Mulliken, NPA (natural population analysis), and CHelpG (electrostatic potential charges from electrostatic potentials generalized) atomic charges were calculated at the MP2/6-31G* level.[19,20] Then, a complex was divided into two parts: TMA and the corresponding aromatic aggregate. Table 4 summarized the calculated charges.

All the three types of atomic charges indicate that charge transfer from TMA to aromatics takes place, suggesting that

TABLE 4: Charge Transfer among TMA and Aromatics at the MP2/6-31G* Level

system	Mulliken	CHelpG	NPA
Figure 1a, benzene−TMA−pyrrole	0.057−0.895−0.048	0.130−0.737−0.134	0.014−0.969−0.016
Figure 1b, benzene−TMA−benzene	0.058−0.885−0.058	0.135−0.730−0.135	0.015−0.970−0.015
Figure 1c, benzene−TMA−indole	0.055−0.898−0.047	0.120−0.715−0.166	0.014−0.971−0.015
Figure 1d, pyrrole−TMA−indole	0.046−0.909−0.046	0.122−0.716−0.163	0.014−0.970−0.015
TMA−pyrrole	0.950−0.050	0.853−0.147	0.983−0.017
TMA−benzene	0.937−0.063	0.853−0.147	0.984−0.016
TMA−indole	0.948−0.052	0.821−0.179	0.984−0.016

TABLE 5: Morokuma Decomposition Analysis on Binding Energy at the HF/6-31+G//MP2/6-31G** Level**

system	ES	EX	PL	CT	MIX	BSSE	ΔE (ΔE^{BSSE})
Figure 1a, benzene−TMA−pyrrole	−16.85	12.95 (13.56)	−3.73	−6.58 (−5.99) [55.5]	0.99 (2.22)	2.43	−13.22 (−10.79)
Figure 1b, benzene−TMA−benzene	−14.16	12.35 (12.94)	−3.48	−7.06 (−6.46) [72.3]	1.05 (2.23)	2.36	−11.29 (−8.93)
Figure 1c, benzene−TMA−indole	−18.92	16.91 (17.50)	−4.72	−7.21 (6.48) [62.0]	1.07 (2.17)	2.42	−12.88 (−10.45)
Figure 1d, pyrrole−TMA−indole	−21.35	16.97 (17.57)	−4.87	−6.97 (−6.19) [49.0]	1.01 (2.22)	2.56	−15.20 (−12.64)
TMA−pyrrole	−10.40	7.95 (8.26)	−2.25	−3.54 (−3.15) [47.1]	0.37 (1.07)	1.39	−7.87 (−6.47)
TMA−benzene	−7.33	6.50 (6.81)	−1.87	−3.69 (−3.39) [71.7]	0.42 (1.05)	1.24	−5.97 (−4.73)
TMA−indole	−12.24	10.79 (11.11)	−3.13	−3.96 (−3.51) [51.5]	0.38 (0.97)	1.36	−8.16 (−6.81)

TABLE 6: Decomposition Analysis on the Interaction between π1 and π2 in π1−TMA−π2 Sandwich Complexes at HF/6-31+G//MP2/6-31G* Level**

system	ΔE (ΔE^{BSSE})	BSSE	ES	EX	PL	CT	MIX	$d(\pi-\pi)$
Figure 1a, benzene-pyrrole	+0.19 (0.19)	0.00	0.20	0.00 (0.00)	0.00	0.00 (0.00)	0.00 (0.00)	4.86
Figure 1b, benzene-benzene	+0.23 (0.24)	0.01	0.24	0.00 (0.00)	0.00	−0.01 (0.00)	0.00 (0.00)	4.35
Figure 1c, benzene-indole	+0.33 (0.48)	0.15	0.42	0.04 (0.06)	−0.02	−0.12 (−0.05)	0.00 (0.06)	3.33
Figure 1d, pyrrole-indole	+0.32 (0.35)	0.02	0.35	0.00 (0.00)	−0.01	−0.02 (0.00)	0.00 (0.00)	4.16

charge transfer is involved in the binding of TMA to the two aromatics. Furthermore, although different algorithms release different values, the amount of the transferred charge between the TMA and a π system in a sandwiched π−TMA−π is similar to the amount observed in the corresponding TMA−π complex (Table 4) no matter what method was employed in the calculation. This result demonstrates that the additivity also exists in charge transfer. Among the three types of atomic charges, CHelpG has the biggest value and NPA is the smallest. Notably, the sum of the calculated NPA atomic charges on TMA is almost the same as in different sandwich complexes with a value of 0.970 atomic units.

3.4. Morokuma Decomposition Analysis on Binding Energy. To understand deeply the intermolecular interaction among TMA and aromatics, such as the contributions from electrostatic interaction, polarization and charge-transfer interaction, Morokuma decomposition analysis[21] on the binding energy was performed on the sandwich complexes at the HF/6-31+G** level on the basis of MP2/6-31G* optimized structures. The sandwich complexes were divided into two parts: TMA and the aggregate of the two aromatics, corresponding to monomer 1 and monomer 2 for the software GAMESS. The calculated results were summarized in Table 5, in which the ES, EX, PL, CT, MIX, BSSE, and ΔE denote electrostatic, exchange repulsion, polarization, charge transfer, high order coupling, basis set superposition error, and total binding energies, respectively. The data in parentheses in Table 5 stand for the overall binding energies corrected by BSSE that is estimated with the software GAMESS as well, and the data in brackets are the percentages of the BSSE corrected CT over the BSSE corrected overall binding energy.

Table 5 shows that ES, CT, and PL energies are always favorable to the binding between TMA and aromatics. Among them, the ES is the most important binding component. But, it was also observed that the CT, which contributes at least about 49% of the overall binding energy, is more important than PL. Furthermore, the BSSE corrected CT energies in different sandwich complexes range from 6.0 to 6.5 kcal/mol, suggesting no significant difference in charge-transfer energy in different complexes. This is in agreement with the calculated NPA atomic charges on TMA, which are almost the same as in different sandwiches (Table 4). Therefore, the atomic charges calculated with NPA algorithm might be more reasonable for our systems than CHelpG. On the other hand, Table 5 shows that exchange repulsion and high order coupling are always unfavorable to the binding between TMA and aromatics. The main obstacle to the binding comes from exchange repulsion, according to the decomposition results (Table 5). The binding between TMA and benzene, either in the π−TMA−π or in TMA−π complexes, has its characteristic that the charge transfer with a percentage of about 72% over the ΔE^{BSSE} plays a more important role than in other complexes such as in the complexes of TMA−pyrrole or pyrrole−TMA−indole (Table 5). This could be attributed to the fact that pyrrole or indole contains a nitrogen atom with higher electronagtivity than carbon atoms in benzene. Therefore benzene should be easier to transfer its π electrons to TMA than pyrrole or indole, resulting in greater CT energy in the binding of TMA with benzene in either the π−TMA−π or TMA−π complexes. Indeed, TMA−pyrrole has the smallest CT contribution in its binding energy (Table 5). Another interesting observation is that the CT contribution to ΔE^{BSSE}, in terms of percentage, in the complex π1−TMA−π2 roughly equals to an average of the two corresponding percentages in the complexes TMA−π1 and TMA−π2 (Table 5). This result might be helpful for modifying the existing conventional force fields in reproducing the binding strength in the complexes of TMA−π or in π−TMA−π.

A many-body interaction is involved in π−TMA−π complexes. However, our Morokuma decomposition was carried out on the basis of two monomers: TMA and aromatic aggregate. To study the interaction between the two aromatics, Morokuma decomposition was employed again to analyze the interaction between them in the sandwich π−TMA−π complex at the same HF/6-31+G**//MP2/6-31G* level, Table 6. According to the analysis result in Table 6, it was found that there is a weak electrostatic repulsion between two aromatics with a value of less than 0.4 kcal/mol. All the other interactions, such as EX, PL, CT, and MIX, do not exist or are negligible with an error

less than 0.1 kcal/mol. This result suggests that the interaction between two aromatics in π−TMA−π sandwiches does not need to be taken into account. It could be attributed to the long interaction distance between the two aromatics, $d(\pi-\pi)$ in Table 6. The shortest $d(\pi-\pi)$ is 3.3 Å in the complex benzene−TMA−pyrrole, which corresponds to the strongest BSSE corrected interaction energy of 0.48 kcal/mol, whereas the longest distance is 4.86 Å in the complex benzene−TMA−pyrrole, which has the weakest BSSE corrected interaction energy of 0.19 kcal/mol.

4. Conclusion

In conclusion, our study on the π−cation−π sandwiches of TMA with benzene, pyrrole, and indole revealed additivity of both the geometries and the binding energies. The preferred structure of such a complex can be obtained by merging the corresponding TMA−π complexes via the cation. The binding energies of the π−TMA−π sandwiches are the sums of the two corresponding TMA−π systems. Thus, it may be expected that the interaction of a choline moiety with two Trp residues, which can be mimicked by the interaction of TMA with two indole rings that are as strong as ca. −19 kcal/mol in a vacuum, should significantly consolidate the stability of the novel solenoid fold of LytA under physiological conditions.[4] The contribution of electron correlation to the overall binding energy was estimated to be at least 53%, with dispersion serving as the main component of the electron correlation interaction. Furthermore, the calculated BSSE and ΔZPE also demonstrated the additivity that the BSSE and ΔZPE for a π−TMA−π sandwich could be estimated as the sum of the BSSEs and ΔZPEs of two corresponding stand-alone TMA−π complexes. Therefore, our demonstration of geometrical and energetic additivity thus provides a convenient and effective way to construct π−TMA−π sandwiches and to estimate their binding energies. The electrostatic, charge transfer, and polarity always impel the binding between TMA and aromatics, whereas the exchange repulsion and high order coupling always hamper TMA approaching aromatics. Both the transferred NPA atomic charge and charge-transfer energy remain almost unchanging in different complexes of TMA−π or π−TMA−π. The interaction between the 2 aromatics in a sandwich π−TMA−π complex is negligible for their long interaction distance. All these results, in turn, should be helpful in the development of force fields representing such interactions of this type for application to biological systems.

Acknowledgment is made of grants from the National Natural Science Foundation of China (29725203 and 20072042), the State Key Program of Basic Research of China (2002CB512802), the 863 Hi-Tech Program (2001AA235051and 2001AA235041), and the Life Science Foundation for Young Scientists of the Chinese Academy of Science (STZ-00-06)

Supporting Information Available: Figure S1. Twelve selected initial structures of π−cation−π complexes. Figure S2. Normal mode analysis on indole−TMA−benzene. Figure S3. New normal mode of indole−TMA−benzene. This material is available free of charge via the Internet at http://pubs.acs.org.

References and Notes

(1) Ma, J. C.; Doughterty, D. A. *Chem. Rev.* **1997**, *97*, 1303.
(2) Dougherty, D. A. *Science* **1996**, *271*, 163.
(3) Sussman, J. L.; Harel, M.; Frolow, F.; Oefner, C.; Goldman, A.; Toker, L.; Silman, I. *Science* **1991**, *25*, 872.
(4) Fernandez-Tornero, C.; Lopez, R.; Garcia, E.; Gimenez-Gallego, G.; Romero, A. *Nature Struct. Biol.* **2001**, *8*, 1020.
(5) Aleshin, A. E.; Firsov, L. M.; Honzatko, R. B. *J. Biol. Chem.* **1994**, *269*, 15631.
(6) (a) Doyle, A. D.; Cabral, M. J.; Pfuetzner, A. R.; Kuo, A.; Gulbis, M. J.; Cohen, L. S.; Chait, T. B.; MacKinnon, R. *Science* **1998**, *280*, 69. (b) French, J. R.; Shoukimas, J. J. *Biophys. J.* **1981**, *34*, 271.
(7) Burley, S. K.; Petsko, G. A. *Adv. Protein Chem.* **1988**, *39*, 125.
(8) Pullman, A.; Berthier, G.; Savinelli, R. J. *J. Am. Chem. Soc.* **1998**, *120*, 8553.
(9) Kim, K. S.; Lee, J. Y.; Lee, S. J.; Ha, T. K.; Kim, D. H. *J. Am. Chem. Soc.* **1994**, *116*, 7399.
(10) Zhu, W.; Tan, X.; Puah, C. M.; Gu, J.; Jiang, H.; Chen, K.; Felder, E. C.; Silman, I.; Sussman, J. J. *J. Phys. Chem. A* **2000**, *104*, 9573.
(11) Tan, X.; Zhu, W.; Cui, M.; Luo, X.; Gu, J.; Silman, I.; Sussman, J. L.; Jiang, H.; Chen, K. *Chem. Phys. Let.* **2001**, *349*, 113.
(12) Liu, T.; Gu, J.; Tan, X.; Zhu, W.; Luo, X.; Jiang, H.; Chen, K.; Silman, I.; Sussman, J. L. *J. Phys. Chem. A* **2001**, *105*, 5431.
(13) Boys, S. F.; Bernardi, F. *Mol. Phys.* **1970**, *19*, 553.
(14) Frisch, M. J.; Trucks, G. W.; Schlegel, H. B.; Scuseria, G. E.; Robb, M. A.; Cheeseman, J. R.; Zakrzewski, V. G.; Montgomery J. A., Jr.; Stratmann, R. E.; Burant, J. C.; Dapprich, S.; Millam, J. M.; Daniels, A. D.; Kudin, K. N.; Strain, M. C.; Farkas, O.; Tomasi, J.; Barone, V.; Cossi, M.; Cammi, R.; Mennucci, B.; Pomelli, C.; Adamo, C.; Clifford, S.; Ochterski, J.; Petersson, G. A.; Ayala, P. Y.; Cui, Q.; Morokuma, K.; Malick, D. K.; Rabuck, A. D.; Raghavachari, K.; Foresman, J. B.; Cioslowski, J.; Ortiz, J. V.; Stefanov, B. B.; Liu, G.; Liashenko, A.; Piskorz, P.; Komaromi, I.; Gomperts, R.; Martin, R. L.; Fox, D. J.; Keith, T.; Al-Laham, M. A.; Peng, C. Y.; Nanayakkara, A.; Gonzalez, C.; Challacombe, M.; Gill, P. M. W.; Johnson, B. G.; Chen, W.; Wong, M. W.; Andres, J. L.; Head-Gordon, M.; Replogle, E. S.; Pople, J. A. *Gaussian 98*, Revision A.7; Gaussian, Inc.: Pittsburgh, PA, 1998.
(15) Accelrys ViewerPro Trial Edition Version 5.0, 6/12/2002, Accelrys Inc., www.accelrys.com.
(16) Felder, C.; Jiang, H. L.; Zhu, W. L.; Chen, K. X.; Silman, I.; Botti, S.; Sussman, L. J. *J. Phys. Chem. A* **2001**, *105*, 1326
(17) Head-Gordon, M.; Pople, J. A.; Frisch, M. J. *Chem. Phys. Lett.* **1988**, *153*, 503.
(18) Rappe, A. K.; Bernstein, E. R. *J. Phys. Chem. A* **2000**, *104*, 6117.
(19) Reed, A. E.; Curtiss, L. A.; Weinhold, F. *Chem. Rev.* **1988**, *88*, 899.
(20) Breneman, C. M.; Wiberg, K. B. *J. Comput. Chem.* **1990**, *11*, 361.
(21) Kitaura, K.; Morokuma, K. *Int. J. Quantum Chem.* **1976**, *10*, 325−340.